

A STUDY ON THAUMASITE FORM OF SULFATE ATTACK (TSA) USING XRD, TG AND SEM

*A. Skaropoulou, G. Kakali and S. Tsivilis**

National Technical University of Athens, School of Chemical Engineering, 9 Heron Polytechniou St., 15773 Athens, Greece

The thaumasite form of sulphate attack (TSA) concerns cements and concretes containing limestone and is attributed to the formation of thaumasite. This work deals with the confirmation of thaumasite formation in cement mortars. Three types of cement were examined: Portland cement and Portland limestone cement containing 15 and 30% mass/mass limestone. The specimens were cured at 5°C, for 12 months, in a 1.8% MgSO₄ solution. The formation of thaumasite was checked and confirmed by XRD, TG and SEM. It was concluded that mortars containing limestone suffer from TSA at low temperature. The combination of XRD, TG and SEM leads to the positive identification of thaumasite and resolves the well known problem of thaumasite and ettringite confusion.

Keywords: identification, Portland limestone cement, sulfate attack, thaumasite

Introduction

It is generally accepted that conventional sulfate attack of cementitious materials involves the formation and the expansive properties of ettringite. However, another kind of sulfate attack, concerning cements and concretes containing limestone and attributed to the formation of thaumasite has been widely discussed during the last years [1–3]. This kind of sulfate attack is of great importance, as the limestone is widely used as filler or as main cement constituent for many years due to its technical and economical advantages. In addition, the new European Standard EN 197-1 (2000) identifies Portland limestone cements that may contain limestone as main constituent, in percentages ranging from 6 to 35% [4].

The formation of thaumasite (CaSiO₃·CaCO₃·CaSO₄·15H₂O) is the result of sulfate attack at low temperature. Thaumasite formation requires a source of calcium silicate, sulfate and carbonate ions, excess humidity and low temperature. It may also be connected with the prior formation of ettringite or the presence of some reactive alumina. Since the formation of thaumasite involves the reaction of C–S–H with carbonate and sulfate ions, it may well take place in ordinary Portland cement (carbonate ions can originate from fine limestone aggregates or extended atmospheric carbonation) or even in sulfate resisting Portland cements [5–14].

The problem of Thaumasite form of Sulfate Attack (TSA) has been discussed during the last years because it has been identified in UK, USA, Canada, South Africa, France, Germany, Norway, Denmark,

Switzerland, Italy and Slovenia and is particularly prevalent in buried concrete. This form of sulfate attack completely destroys the cementitious binding ability of the concrete by transforming it into a mush.

The mechanism and factors affecting thaumasite formation have not been yet fully clarified. Besides its similarities with other hydrated compounds, found in cement and concrete, hinder its positive identification [3]. This work deals with the thaumasite formation in cement mortars and the application of the appropriate analytical techniques for its positive identification.

Experimental

Portland cement clinker of industrial origin and limestone (L) of high calcite content (CaCO₃; 95.7%) were used. The chemical composition of the above materials is presented in Tables 1 and 2 respectively. Portland limestone cements, containing 15 and 30% mass/mass% limestone, were produced by inter-grinding clinker, limestone and gypsum in a pro-pilot plant ball mill of 5 kg capacity. The codes, the composition and the specific surface of the produced cements are given in Table 3.

Mortars were prepared, using the cements of Table 3, (*w/c*=0.5, cement:sand=1:2.50). Siliceous (s) and calcareous (c) sand have been used and mortar prisms of size 40·40·53 mm were prepared. The specimens were air cured for 24 h, then were water-cured for 6 days and finally they were air-cured for 21 days at laboratory temperature (25±2°C). After the 28-day curing the specimens were stored in 1.8% MgSO₄ so-

* Author for correspondence: stsiv@central.ntua.gr

Table 1 Chemical and mineralogical composition of clinker

Chemical composition/%									
SiO ₂	Al ₂ O ₃	Fe ₂ O ₃	CaO	MgO	K ₂ O	Na ₂ O	SO ₃	TOTAL	fCaO
21.47	5.00	3.89	65.67	1.89	0.68	1.16	1.04	99.70	1.15
Mineralogical composition/%									
*C ₃ S	C ₂ S	C ₃ A	C ₄ AF	LSF	SR	AR	HM		
65.0	12.6	6.7	11.8	0.958	2.42	1.29	2.18		

*Cement chemistry notation: C=CaO, S=SiO₂, A=Al₂O₃, F=Fe₂O₃

Table 2 Chemical analysis of limestone (%)

SiO ₂	Al ₂ O ₃	Fe ₂ O ₃	CaO	MgO	K ₂ O	LOI
0.54	0.43	0.20	53.61	1.29	0.06	43.73

Table 3 Codes and composition of the produced mixes

Code	Composition of samples
PC	Clinker 100% (gypsum: 5% of clinker mass)
LC1	Clinker 85, limestone 15 mass/mass% (gypsum: 5 mass/mass% of clinker mass)
LC2	Clinker 70, limestone 30 mass/mass% (gypsum: 5 mass/mass% of clinker mass)

lution. The samples were cured at 5°C (laboratory refrigerator, ±2°C) and the MgSO₄ solution was replaced every 3 months.

XRD measurements were performed on samples at regular intervals in order to identify any compounds formed during the curing. A Siemens D-5000 X-ray diffractometer, with CuK_α radiation ($\lambda = 1.5405 \text{ \AA}$) was used. Measurements were carried out on samples coming from either the hard core or the deteriorated part of the specimens. In addition, thermogravimetric analysis (TG-DTG) was applied in order to detect small amounts of compounds. A Mettler Toledo TG/SDTA 851 instrument was used. The samples (~20 mg) were heated from 20 to 600°C at a constant rate of 5°C min⁻¹, in an atmosphere of carbon dioxide free nitrogen, flowing at 50 cc min⁻¹. Finally, deteriorated surfaces of selected samples were examined using a JEOL JSM-5600 Scanning Electron Microscope. An OXFORD LINK ISIS 300 Energy dispersive X-ray spectrometer (EDXS) was used in order to observe the composition of various phases (accelerating voltage: 20 kV, beam current: 0.5 nA).

Results and discussion

The identification of products formed as a result of sulfate attack was based on XRD and DTG measurements. In all cases, the composition of the intact core of the specimens corresponded to that of a normal hy-

drated cement containing mainly calcite as well as calcium hydroxide and ettringite.

In the specimens which suffered from cracking and expansion, measurements were also carried out on the soft, white material covering the surface of the cracks. In all cases, this material was found to contain mainly thaumasite, gypsum and traces of brucite. The XRD patterns of the samples PC-c, LC1-s and LC2-s are indicatively presented in Fig. 1. In addition to the peaks corresponding to the aggregates, the characteristic peaks of thaumasite and gypsum are clearly seen. Thaumasite belongs to the ettringite-like group of minerals and this results in very similar XRD patterns. The possible formation of thaumasite-ettringite solid solutions makes the positive identification more complex. The identification of thaumasite was mainly

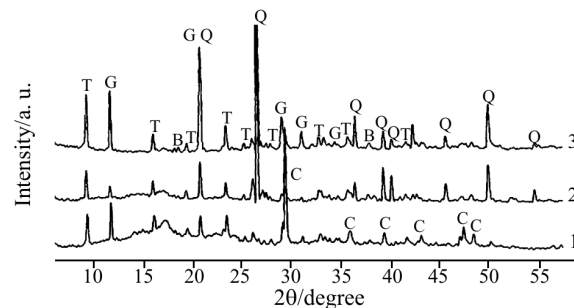


Fig. 1 XRD patterns of deterioration products at 5°C.
(1: PC-c, 2: LC1-s, 3: LC2-s) (T: thaumasite,
G: gypsum, B: brucite, Q: quartz, C: calcite)

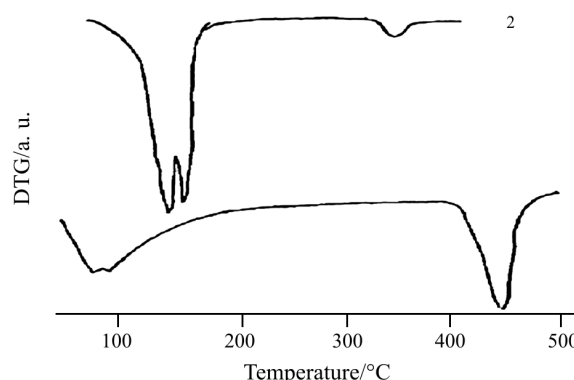


Fig. 2 DTG curves of the sample LC2-c (1: intact core,
2: degradation products)

based on the peaks (20) at around 16, 23.5 and 28°, which are absent from the ettringite pattern. The absence of ettringite was confirmed by the absence of its characteristic peaks at around 15.8, 18.9, 22.9 and 25.5°. The peaks attributable to brucite were too weak to allow a positive identification but its formation was confirmed based on DTG curves. There was no indication of any $\text{Ca}(\text{OH})_2$ in these samples. The interesting point is that thaumasite was found even in the PC sample which does not contain limestone as cement main constituent. In this case, it seems that the source of CO_3^{2-} ions, required for the formation of thaumasite, is the fine particles of the calcareous aggregates.

Thermoanalytical methods, and especially TG/DTG, have been widely used for the study of cement hydration, since the total mass loss of cement pastes is a measure of the rate of hydration, while any changes of the number and shape of peaks indicate changes of the stoichiometry in the hydrated products [15–18]. Figure 2 presents the DTG curve of degradation products from samples LC2-c in relation to the DTG curve of the hard core of same sample. The double peak in the range 100–130°C can be associated with the dehydration of thaumasite and gypsum. The dehydration of ettringite and other hydration products, unaffected by sulfate attack, takes place at

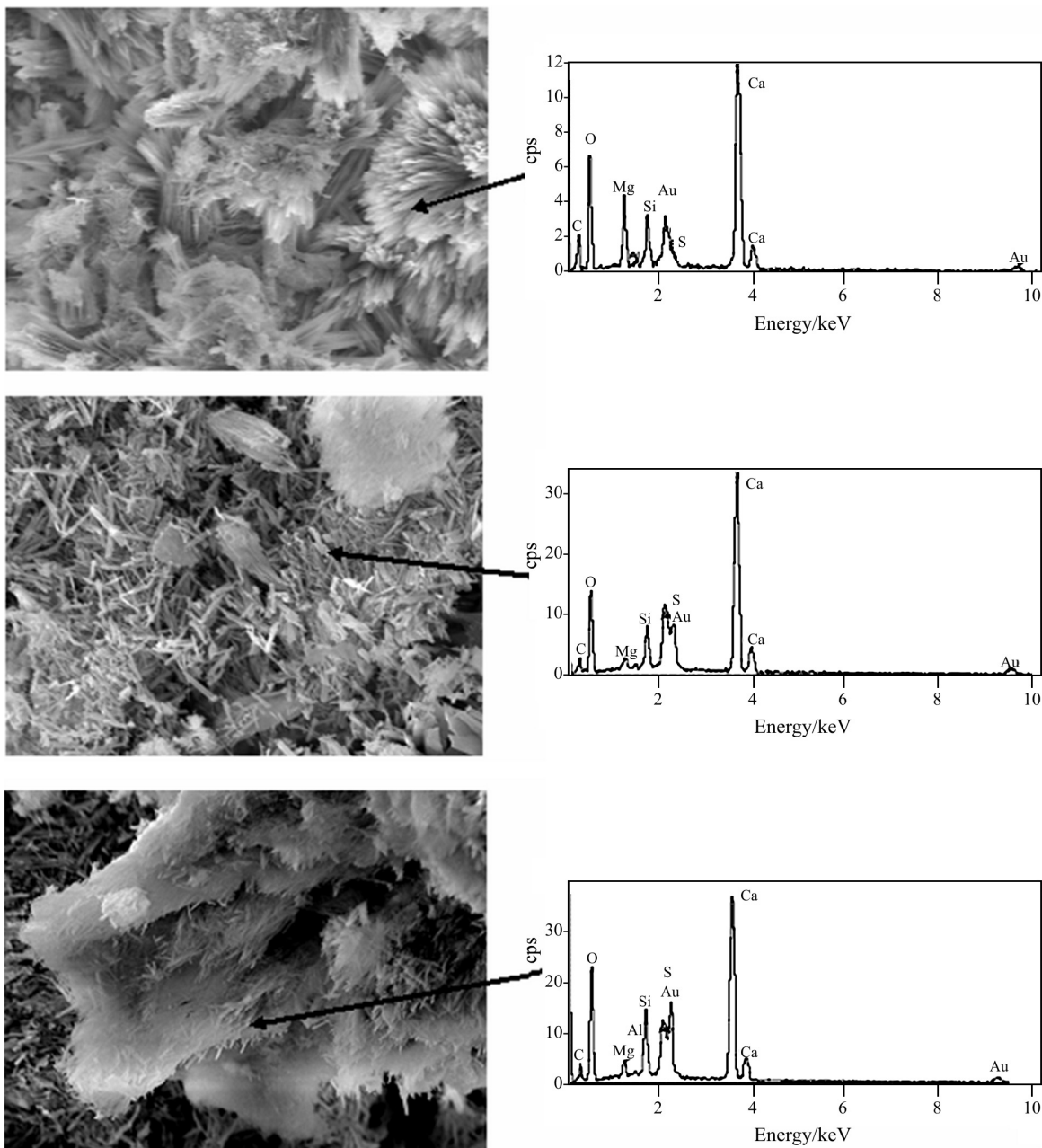
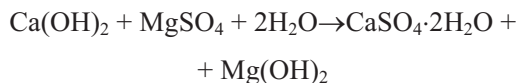


Fig. 3 SEM photos of sample PC (a – intact core of PC-s, b – damaged area of PC-c, c – damaged area of PC-c)

lower temperature as confirmed by the curve of the intact sample. It is clearly seen that degraded sample also contains small amounts of brucite (small peak at around 350–400°C), and no portlandite at all.

The coexistence of gypsum and brucite, in combination with the absence of portlandite, leads to the conclusion that portlandite, most probably, has reacted with magnesium sulfate to form gypsum and brucite, according to the equation:



The very low solubility of brucite shifts the above reaction to the right and favors the consumption of calcium hydroxide. This leads to a pH reduction and as a result C–S–H becomes more susceptible to sulfate attack.

Figure 3 presents three SEM photos of the PC samples. Photo 3a is a representative image of the intact core in the sample PC-s. The predominating phase is in the form of elongated rod-shaped particles radiating outwards. The microanalysis of these particles showed that they consist mainly of Ca, Si and O, therefore they belong to the C–S–H phase of hydrated cement which is the product of the hydration reactions of the calcium silicate compounds. The presence of Mg²⁺ ions is probably due to the diffusion of these ions through the pore solution of the sample. Photo 3b shows the white soft material that covers the damaged area of the sample PC-c and has a needle-like texture. The needles are approximately 2 microns long and 0.5 microns wide. The microanalysis showed that the needles consist mainly of Ca, S, Si and O. There are traces of Mg and no detectable amount of Al. The ratio Ca:S:Si is close to 3:1:1. These observations, along with the XRD pattern, strongly suggest that this needle-like material is thaumasite. Photo 3c is from another area of the same sample. It shows these tiny needles growing on the surface of a calcite grain, which seems to be the source of the carbonate ions necessary for the formation of thaumasite.

Figure 4 presents two SEM photos from the deterioration products of sample LC2-s. The microanalysis of the needle-like material that covers the degraded areas confirms the presence of thaumasite.

The results drawn from each one of the above monitoring techniques are in good accordance with each other. It was confirmed that limestone cements suffer from the thaumasite form of attack at low temperature to an extent proportional to the limestone content. The interesting point is that the use of calcareous aggregates results in thaumasite formation even in PC mortars, when the appropriate conditions prevail.

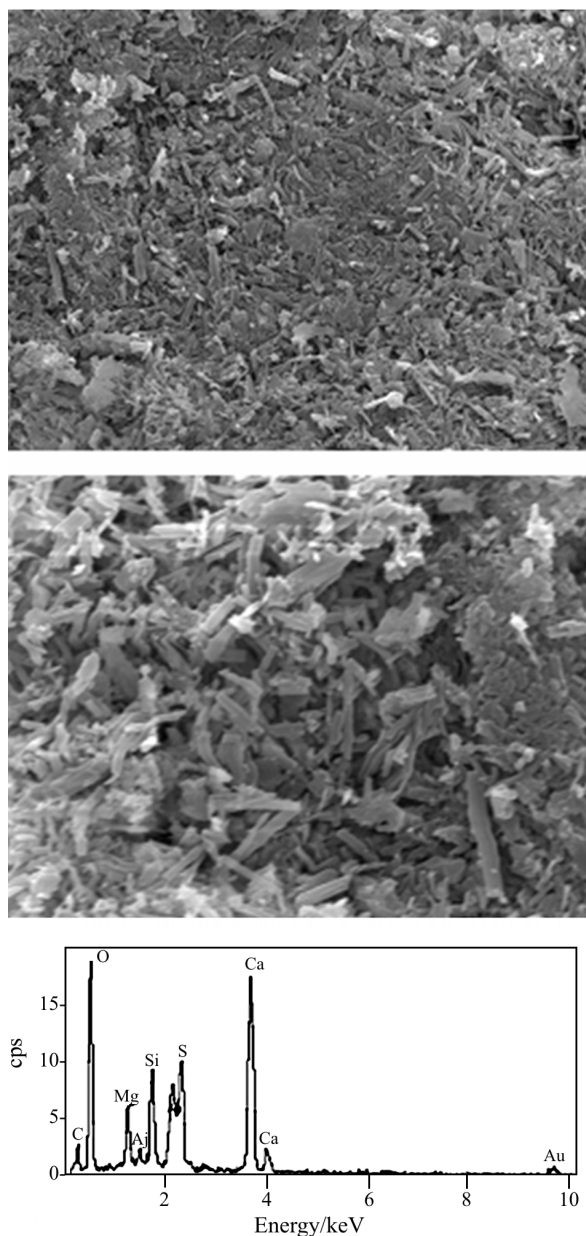


Fig. 4 SEM photos of sample LC2-s (damaged area)

Conclusions

From the present study the following conclusion can be drawn:

- Mortars containing limestone, either as cement main constituent or as sand, suffer from the thaumasite form of sulfate attack at low temperature.
- Thaumasite formation is accompanied by the formation of brucite and secondary gypsum, while calcium hydroxide is a reactant, rather than a product of the sulfate-attack reaction.
- The combination of XRD, TG and SEM leads to the positive identification of thaumasite and resolves the well known problem of thaumasite and ettringite confusion.

References

- 1 P. W. Brown, *Cem. Concr. Compos.*, 24 (2002) 301.
- 2 J. Bensted, *Cem. Concr. Compos.*, 21 (1999) 117.
- 3 R. N. Swamy, *Cem. Concr. Compos.*, 21 (1999) iii.
- 4 European Committee for Standardization, EN 197-1, EN/TC51/WG 6 rev., 2000.
- 5 M. E. Gaze and N. J. Crammond, *Cem. Concr. Compos.*, 22 (2000) 209.
- 6 J. Aguilera, M. T. Blanco Varela and T. P. Vazquez, *Cem. Concr. Res.*, 31 (2001) 1163.
- 7 P. Brown, R. D. Hooton and B. Clark, *Cem. Concr. Compos.*, 26 (2004) 993.
- 8 I. Sims and S. A. Huntley, *Cem. Concr. Compos.*, 26 (2004) 837.
- 9 D. E. Macphee and S. J. Barnett, *Cem. Concr. Res.*, 34 (2004) 1591.
- 10 G. Collett, N. J. Crammond, R. N. Swamy and J. H. Sharp, *Cem. Concr. Res.*, 34 (2004) 1599.
- 11 S. M. Torres, C. A. Kirk, C. J. Lynsdale, R. N. Swamy and J. H. Sharp, *Cem. Concr. Res.*, 34 (2004) 1297.
- 12 G. Kakali, S. Tsivilis, A. Skaropoulou, J. H. Sharp and R. N. Swamy, *Cem. Concr. Compos.*, 25 (2003) 987.
- 13 S. Tsivilis, G. Kakali, A. Skaropoulou, J. H. Sharp and R. N. Swamy, *Cem. Concr. Compos.*, 25 (2003) 979.
- 14 S. A. Hartshorn, R. N. Swamy and J. H. Sharp, *Advances in Cement Research*, 13 (2001) 31.
- 15 E. T. Stepkowska, J. L. Perez-Rodriguez, M. C. Jimenez de Haro and M. J. Sayagues, *J. Therm. Anal. Cal.*, 69 (2002) 187.
- 16 W. Roszczynalski, *J. Therm. Anal. Cal.*, 70 (2002) 387.
- 17 Z. Giergiczny, *J. Therm. Anal. Cal.*, 76 (2004) 747.
- 18 I. A. Ibrahim, H. H. ElSersy, M. F. Abadir, *J. Therm. Anal. Cal.*, 76 (2004) 713.

DOI: 10.1007/s10973-005-7198-2